

Small recoil momenta double ionization of He and two-electron ions by high energy photons

M. Ya. Amusia^{1,2}, E. G. Drukarev³, E. Z. Liverts¹

¹ *Racah Institute of Physics, The Hebrew University
Jerusalem 91904 Jerusalem, Israel*

² *A. F.Ioffe Physical-Technical Institute,
St. Petersburg 194021, Russia*

³ *National Research Center "Kurchatov Institute"*

*B. P. Konstantinov Petersburg Nuclear Physics Institute
Gatchina, St. Petersburg 188300, Russia*

Abstract

We calculate various differential and double differential characteristics of ionization by a single photon for H^- , He and for the two-electron ions with $Z = 3, 4, 5$ in the region of the so-called quasi-free mechanism (QFM) domination. We employ highly accurate wave functions at the electron-electron coalescence line where coordinates of both ionized electrons coincide. We trace the Z dependence for the double differential distribution. For all considered targets we discuss the dependence of the photoelectron energy distribution on the photon energy. Our calculation demonstrated the rapid decrease of QFM contribution with increase of the difference in energy of two outgoing electrons, and with decrease of the angle between two outgoing momenta. As a general feature, we observe the decrease of QFM contribution with nuclear charge growth.

PACS numbers:

I. INTRODUCTION

By "high energy photoionization" we mean absorption of photons with energies ω much exceeding the single particle electron binding energies I , i.e. $\omega \gg I$. If only one photoelectron is emitted, the momentum transferred to the nucleus that is called the recoil momentum q , is estimated as $q \approx p$ with p being the momentum of the photoelectron. Thus, the recoil momentum strongly exceeds the characteristic binding momentum of the ionized object $\mu = (2mI)^{1/2}$ with m being the electron mass (we employ the relativistic system of units with $\hbar=1$, $c = 1$), i.e. $q \gg \mu$. This is because photoionization with only one electron knocked out cannot take place on a free electron.

Similar situation takes place for the double photoionization, it is in emission of two electrons by a single photon, while the photon energy ω is not too large. The sharing of energy is strongly unequal and $q \approx p_1 \approx (2m\omega)^{1/2}$ with p_1 standing for momentum of the faster photoelectron, while the second electron is emitted with momentum $p_2 \sim \mu$. However, with the increase of ω the role of so-called quasi-free mechanism (QFM) suggested in [1] becomes more and more important. In the frame of QFM momenta of photoelectrons $\mathbf{p}_{1,2}$ and that of the photon \mathbf{k} compose such configuration that the recoil momentum

$$\mathbf{q} = \mathbf{k} - \mathbf{p}_1 - \mathbf{p}_2, \tag{1}$$

becomes as small as the binding momentum μ , i.e.

$$q \sim \mu. \tag{2}$$

Since each act of transfer of large momentum $q \gg \mu$ to the nucleus leads to the small factor $1/q^2$ in the amplitude, the QFM provides surplus in differential characteristics and in the total cross section of double ionization.

Most of the publications on QFM touched the theory of the mechanism for the case of two-electron (helium-like) atomic systems. In the first calculation of the QFM contribution to the total double photoionization cross section [2] it was shown to become the main mechanism of the process at the energies of hundreds keV. The nuclear charge dependence of QFM contribution to the cross section was traced in [3]. It was emphasized in [4] that the description of the QFM requires employing the two-electron bound state wave function $\psi(\mathbf{r}_1, \mathbf{r}_2)$ with the proper analytical behavior on the electron-electron coalescence line $\mathbf{r}_1 = \mathbf{r}_2$.

It should satisfy the known relation between the precise two-electron wave function and its coordinate derivative at the line of zero interelectron distance known as the second Kato condition [5]. The fulfillment of this condition by usually employed in calculations of approximate wave functions is necessary for proper description of QFM since it accounts for the singularity of the Coulomb interelectron interaction. The change of the spectrum curve caused by the QFM with the growth of the photon energy was analyzed in [6]. For more details and references see Ch.9 of the book [7].

It follows from the works mentioned above that for helium the QFM provides a noticeable contribution to the spectrum of photoelectrons starting from the photon energies of about 2 keV. The QFM corrections to the total cross section become noticeable at the photon energies of dozens keV. For heavier two-electron ions the corresponding photon energies become larger. As it stands now, experimental data for such energies are not available.

Although the QFM was discussed in literature during many years, to detect it experimentally remained a challenge till this was done by the group of Dörner [8]. Note that this discovery was made 38 years after its prediction [1] and became possible only after invention of a new experimental technique which enables investigation of the double electron photoionization as a function of recoil momentum q . However, the obtained clear manifestation of the QFM has been detected at much smaller value of the photon energy $\omega = 800$ eV than expected. It was found in [8] that the distribution in momenta q transferred to the final state doubly charged ions in double photoionization of helium has a surplus at small q of the order of 1 – 2 atomic units. However [8] did not contain quantitative results.

An important move mainly in experimental investigation and not only of helium atom but of hydrogen molecule also has been made by the quite recent publication [9]. The development of experimental technique leaves no doubt that investigation of the double electron ionization by a single photon as a function of recoil momentum becomes an important tool in studies of short-range interelectron correlations in atoms, molecules and, perhaps, more complex compounds.

In [9] the double differential distributions $d^2\sigma/d\tau d\beta$ with $\tau = \mathbf{p}_1\mathbf{p}_2/p_1p_2$ and

$$\beta = \frac{|\epsilon_1 - \epsilon_2|}{E}, \quad (3)$$

($\epsilon_{1,2}$ are the energies of the photoelectrons, $E = \epsilon_1 + \epsilon_2 = \omega - I^{++}$, where I^{++} is the two-electron ionization potential) have been measured for He atom and H₂ molecule. Quite a

powerful QFM peak at $\tau = -1$, $\beta = 0$ have been observed in both objects. Also the peak in the energy distribution

$$\frac{d\sigma}{d\beta} = \int_{(p_1-p_2)^2}^{(p_1+p_2)^2} \left(\frac{d^2\sigma}{dq^2 d\beta} \right) d(q^2)$$

for the same targets attributed to QFM have been seen.

These results prompt theoretical investigation of QFM for other, not yet investigated two-electron systems that can become the objects of photoionization studies soon. Note that the results of [8] stimulated us to calculate the differential distributions of the process for He atom at $q \sim \mu$ and photon energies $\omega \approx 1$ keV [10]. In [10] we employed approximate bound state wave functions at the electron-electron coalescence line obtained in the work [11]. This enabled us to carry out analytical calculations.

Since then the ability to calculate improved considerably. So, in the present paper, we employ much more sophisticated bound state wave functions [12],[13] having in mind the impressive increase in experimental accuracy achieved in [9]. We also extend our calculations to include all the lightest two-electron positive ions ($Z \leq 5$) and the negative hydrogen ion H^- . For He atom we trace the dependence of the double differential distributions on the photon energy ω . Including several two-electron ions, we trace the Z dependence of the double differential contributions for photon energies around 1 keV.

While we consider the photon energies corresponding to nonrelativistic photoelectrons, i.e. $\omega \ll m$, the QFM is possible only in the vicinity of the center of the energy distribution, where the relative difference of the electron energies β is small, $\beta \ll 1$. The actual value of $\varepsilon_1 - \varepsilon_2$ where the QFM is possible depends on the ratio k/μ of the photon momentum $k = \omega$ and of the characteristic moment of the bound state μ [1]. We consider the case $\omega \ll \mu$. For helium this means $\omega \ll 6$ keV. In this case $p_1 - p_2 \leq q$ and the QFM is at work if

$$\beta \leq \sqrt{\frac{q^2}{mE}} \quad (4)$$

Condition (2) requires also that the photoelectrons move in approximately opposite directions since $\tau = \mathbf{p}_1 \mathbf{p}_2 / p_1 p_2 = (q^2 - p_1^2 - p_2^2) / (2p_1 p_2) \approx -1$.

An important feature of the QFM is that its amplitude F can be expressed in terms of the amplitude F_0 that represent moving to continuum due to the photon absorption by two free electrons at rest-see below and [7]. This explains the name "quasifree"- the two-electron

system can move almost without noticing the nucleus. However to do this the motion of the electrons should be strongly correlated.

One can see that the QFM is impossible in the dipole approximation where we must put $\mathbf{k} = 0$. Thus the photoelectrons move exactly back-to-back with $\mathbf{p}_1 + \mathbf{p}_2 = 0$. The incoming photon carries spin $S = 1$ while the two-electron system in spin singlet state can not carry angular momentum $J = 1$. Thus, we must include the quadrupole terms of interaction between the photon and electrons.

Presenting $\varepsilon_2 = (\mathbf{p}_1 - \mathbf{q})^2/2m$ we find for the differential cross section corresponding to the QFM

$$d\sigma = 2\pi\delta\left(E - 2\varepsilon_1 - \frac{p_1 q_z}{m} - \frac{q^2}{2m}\right) |F|^2 \frac{d^3 p_1}{(2\pi)^3} \frac{dq^2 dq_z}{4\pi}. \quad (5)$$

Here F is the amplitude describing the QFM mechanism; the averaging over photon polarizations should be carried out. Also, z is the direction of momentum $\mathbf{p}_1 - \mathbf{k}$, and we put $\mathbf{p}_1 - \mathbf{k} \simeq \mathbf{p}_1$ in the argument of the delta-function. Using the delta-function for integration over q_z we obtain for the energy distribution

$$\frac{d^2\sigma}{dq^2 d\beta} = \frac{m^2 E}{2} \int \frac{|F|^2 dt}{(2\pi)^3}; \quad t = \mathbf{p}_1 \mathbf{k} / p_1 k, \quad (6)$$

Another double differential distribution of interest is

$$\frac{d^2\sigma}{dq^2 d\tau} = 2p_1 p_2 \frac{d^2\sigma}{dq^2 d\beta} = m^2 E^3 \int \frac{|F|^2}{(2\pi)^3} dt. \quad (7)$$

Employing these expressions, one can obtain other differential distributions, e.g.

$$\frac{d\sigma}{dq^2} = \int_0^{q/p} d\beta \frac{d^2\sigma}{dq^2 d\beta}; \quad p = (mE)^{1/2}. \quad (8)$$

II. THE QFM AMPLITUDE

We introduce

$$\mathbf{R} = (\mathbf{r}_1 + \mathbf{r}_2)/2; \quad \boldsymbol{\rho} = \mathbf{r}_1 - \mathbf{r}_2, \quad (9)$$

with $\mathbf{r}_{1,2}$ denoting the positions of the two electrons in the rest frame of the nucleus. We present the ground state wave function in terms of these variables

$$\Psi(\mathbf{r}_1, \mathbf{r}_2) = \hat{\Psi}(\mathbf{R}, \boldsymbol{\rho}). \quad (10)$$

It is instructive to start with the QFM amplitude $F^{(0)}$ in which the photoelectrons are described by the plane waves. Thus, the wave function of the photoelectrons is

$$\Psi_{ph}(\mathbf{r}_1, \mathbf{r}_2) = \frac{1}{\sqrt{2}} \left(\psi_{p_1}(\mathbf{r}_1) \psi_{p_2}(\mathbf{r}_2) + \psi_{p_1}(\mathbf{r}_2) \psi_{p_2}(\mathbf{r}_1) \right), \quad (11)$$

with $\psi_{p_j}(\mathbf{r}) = e^{-i\mathbf{p}_j \cdot \mathbf{r}}$. Analysis that employs such a wave function contains all essential physics.

Introducing $\boldsymbol{\kappa} = (\mathbf{p}_1 - \mathbf{p}_2)/2 \approx \mathbf{p}_1$ we write

$$F^{(0)} = \sqrt{2} N(\omega) \int d^3 R d^3 \rho e^{-i\mathbf{q}\mathbf{R} + i(\boldsymbol{\kappa} - \mathbf{k}/2)\mathbf{r}} \left(\frac{i\mathbf{e} \cdot \nabla_\rho}{m} - \frac{i\mathbf{e} \cdot \nabla_R}{2m} \right) \hat{\Psi}(\mathbf{R}, \mathbf{r}) + (\mathbf{p}_1 \leftrightarrow \mathbf{p}_2), \quad (12)$$

Here \mathbf{e} is the photon polarization vector, $N(\omega) = \sqrt{4\pi\alpha/2\omega}$ is the normalization factor of the photon wave function, while $\alpha \simeq 1/137$ is the fine structure constant. Integrating by parts we find that since $\kappa = |\boldsymbol{\kappa}| \gg q$, the first term in the parenthesis on the right hand side dominates, providing

$$F^{(0)} = \sqrt{2} N(\omega) \frac{\mathbf{e}\boldsymbol{\kappa}}{m} \int d^3 R d^3 \rho e^{i\mathbf{q}\mathbf{R} + i(\boldsymbol{\kappa} - \mathbf{k}/2)\mathbf{r}} \hat{\Psi}(\mathbf{R}, \mathbf{r}) + (\mathbf{p}_1 \leftrightarrow \mathbf{p}_2). \quad (13)$$

The integral is determined by $R \sim 1/q \sim 1/\mu$ i.e. the characteristic R are of the order of the size of the bound state. The important values of ρ are much smaller being of the order $1/\kappa \ll 1/\mu$. To pick the quadrupole terms we present the wave function as

$$\hat{\Psi}(\mathbf{R}, \boldsymbol{\rho}) = \hat{\Psi}(R, 0, 0) + \zeta \hat{\Psi}'(R, \zeta, 0)|_{\zeta=0} + \rho \hat{\Psi}'(R, 0, \rho)|_{\rho=0} + 0(\rho^2), \quad (14)$$

with $\zeta = \mathbf{R}\boldsymbol{\rho}$. Substituting this expansion into the integral over ρ in Eq.(12)

$$J(\mathbf{a}, R) = \int d^3 \rho e^{i\mathbf{a}\boldsymbol{\rho}} \hat{\Psi}(\mathbf{R}, \mathbf{r}), \quad (15)$$

with

$$\mathbf{a} = \frac{\mathbf{p}_1 - \mathbf{p}_2 - \mathbf{k}}{2} \quad (16)$$

we see that only the third term on the right hand side of Eq.(14) contributes, providing

$$J(\mathbf{a}, R) = -\frac{8\pi \hat{\Psi}'(R, 0, \rho)|_{\rho=0}}{a^4} = -\frac{4\pi m\alpha}{a^4} \hat{\Psi}(\mathbf{R}, 0). \quad (17)$$

The second equality is due to the second Kato cusp condition [5]

$$\frac{\partial \hat{\Psi}(\mathbf{R}, \boldsymbol{\rho})}{\partial \rho} \Big|_{\rho=0} = m\alpha \hat{\Psi}(\mathbf{R}, \boldsymbol{\rho} = 0)/2.$$

Thus, the amplitude

$$F^{(0)} = \sqrt{2}N(\omega)\frac{\mathbf{e}\boldsymbol{\kappa}}{m} \int d^3R e^{i\mathbf{q}\mathbf{R}} J(\mathbf{a}, R) + (\mathbf{p}_1 \leftrightarrow \mathbf{p}_2) \quad (18)$$

can be written as

$$F^{(0)} = F_0 S(q). \quad (19)$$

Here

$$S(q) = \int d^3r e^{i\mathbf{q}\mathbf{r}} \Psi(\mathbf{r}, \mathbf{r}) = \int \frac{d^3f}{(2\pi)^3} \tilde{\Psi}(\mathbf{q} - \mathbf{f}, \mathbf{f}) \quad (20)$$

describes transfer of momentum \mathbf{q} from the nucleus to the bound electrons. In the lowest order of expansion in powers of I^{++}/ω we put $E = \omega$, and as a result have

$$F_0 = -4\pi\sqrt{2}\alpha N(\omega)\frac{\mathbf{e}\boldsymbol{\kappa}}{a^4} + (\mathbf{p}_1 \leftrightarrow \mathbf{p}_2), \quad (21)$$

the amplitude of the process in which one photon moves the system consisting of two free electrons in spin-singlet state to continuum.

In the lowest (dipole) approximation we must put $\mathbf{k} = 0$ in the factor $1/a^4$ with a defined by Eq.(16). This leads to $F_0 = 0$ and $F^{(0)} = 0$ in agreement with the analysis presented above. The leading nonvanishing contribution is provided by next to leading term of expansion of the factor

$$\frac{1}{a^4} = \frac{1}{m^2 E^2} \left(1 + \frac{2\mathbf{p}_1 \mathbf{k}}{mE} \right). \quad (22)$$

Thus the amplitude of the process on the free electrons is

$$F_0 = -16\pi\sqrt{2}\alpha N(\omega)\frac{(\mathbf{e}\mathbf{p}_1)(\mathbf{p}_1 \mathbf{k})}{m^3 E^3}, \quad (23)$$

while the amplitude for the process on the bound electrons is given by Eq.(19).

Now we describe the photoelectrons by nonrelativistic Coulomb functions. Note that we do not employ expansion in powers of I^{++}/ω . The two-electron wave function is presented by Eq.(11) with

$$\psi_{p_j}(\mathbf{r}) = e^{-i\mathbf{p}_j \mathbf{r}} X_{p_j}(\mathbf{r}); \quad X_{p_j}(\mathbf{r}) = N(p_j) {}_1F_1(i\xi_j, 1, ip_j r - i\mathbf{p}_j \mathbf{r}), \quad (24)$$

where ${}_1F_1(b, 1, z)$ is the confluent hypergeometric function of the first kind, $\xi_j = m\alpha Z/p_j$, $N(p_j) = 2\pi\xi_j/(1 - e^{-2\pi\xi_j}) = \psi_{p_j}(\mathbf{r} = 0)$. Evaluation similar to that carried out for the case when the photoelectrons are described by plane waves [10], [7] provides

$$F = F_0 S_1(q). \quad (25)$$

Here F_0 is given by Eq.(23) while

$$S_1(q) = \int d^3R e^{i\mathbf{q}\mathbf{R}} X_{p_1}(\mathbf{R}) X_{p_2}(\mathbf{R}) \tilde{\Psi}(R, 0), \quad (26)$$

see Eqs. (19), (20). The corrected analytical representation for the integral $S_1(q)$ is presented in the Appendix.

III. DIFFERENTIAL DISTRIBUTIONS

Combining Eqs.(6), (25) and (26) we find for the double differential distribution

$$\frac{d^2\sigma}{dq^2 d\beta} = \frac{2^6}{15} \alpha^3 \frac{\omega |S_1(q)|^2}{m^2 E^3}. \quad (27)$$

Note that the photon energy ω is much larger than the two-electron ionization energy I^{++} . Therefore we used the approximation $E \simeq \omega$ in the real calculations.

In Figs.1 and 2 we trace the Z dependence of the distributions $d^2\sigma/dq^2 d\beta$ and $d\sigma/dq^2$ correspondingly. We present the results for He as well as for H^- and the two-electron ions of the nuclei with $Z = 3, 4, 5$. These distributions were studied in [8] for He only. The horizontal axis is for q^2 . The vertical axis is for $d\sigma/dq^2 d\beta$ in *barns* $\cdot a_0^2$ and for $d\sigma/dq^2$ in barns. In Figs. 1a and 2a we show these distributions for helium at $\omega = 800$ eV (the studies in [8] were carried out for this value of ω). To make comparison for different ions more sensible, for other objects the energies were changed proportionally to the total binding energy I^{++} , that is 0.53, 2.90, 7.28, 13.66, and 22.03 for $Z=1, 2, 3, 4$, and 5, respectively. To have a feeling of dependence of these distributions on the photon energy ω we present them for $\omega = 1000$ eV (in Figs.1b and 2b, in [8]) were carried out for this value of ω in He, and energies for other objects modified accordingly to their respective values of I^{++} . In these figures as well as in Figures 3,4 we change the values of ω for H^- , ($Z = 1$), Li^+ ($Z = 3$), Be^{2+} ($Z = 3$) and B^{3+} ($Z = 5$) proportionally to the total binding energy I^{++} , as compared to that of $\omega = 800(1000)$ eV for He.

As is seen from Fig.1, at equal photoelectron energies the magnitude of the double differential cross section rapidly decreases with recoil momentum growth. The magnitude of it is the smaller the bigger is the nuclear charge. Fig.2 presents the dependence of $d\sigma/d(q^2)$ upon recoil moment. The curves for different Z are similar having a profound maximum and rapidly decreasing in magnitude with increase of Z .

In Figs.3 and 4 we present the double differential distributions $d^2\sigma/d\tau d\beta$ at $\beta = 0$ and the angular distributions $d\sigma/d\tau$ studied in [9] for He atom, respectively. This enables us to trace the Z dependence of the effect. In Fig.3 we compare also the results found by employing the functions on the coalescence line $\tilde{\Psi}(R, 0)$ obtained in [12], [13] with those obtained by using approximate functions suggested in [11]. One can see that the difference is negligible for H^- and for He atom. It increases with Z , remaining very small at least for $Z \leq 5$. Fig 3 demonstrates that the QFM cross-sections are rapidly decreasing with increase of the angle between the outgoing electrons momenta, their magnitudes, as in Fig. 1 and Fig.2, rapidly decrease with Z growth. The results depicted in Fig.4 demonstrate rapid decrease of $d\sigma/d\tau$ with decrease of the angle between the outgoing electrons momenta and growth of Z . In Fig. 5(a-e) we present in details the photoelectron energy distributions $d\sigma/d\beta$ at $\beta = 0$ for ($Z = 1 - 5$). Fig. 5 depicts the dependence of $d\sigma/d\beta$ upon photon energy, showing its rapid monotonic decrease with ω . Note, however, that $d\sigma/d\beta$ is bigger for $Z = 2$, than for $Z = 1$, and the decrease on the way from $Z = 2$ to $Z = 5$ is relatively slow.

This can be useful for extension of the analysis carried out in [9] for another values of the photon energies and for other targets.

IV. SUMMARY

As it was mentioned above, the QFM predicted 45 years ago [1] was beyond the possibilities of experimental investigations for a long time. The work [8] provided experimental evidence of the existence of QFM. Recent publication [9] provided experimental data on the double and single differential distributions for He atom and for H_2 molecule. This enables us to hope that studies of QFM for other targets will take place transforming a couple of experiments into whole domain of research that will present data on short range inter-electron correlations in a whole variety of systems of which He, H^- and other helium-like ions form only a small domain.

The QFM is interesting from several points of view. It probes the wave function between the bound electrons at small distances and provides a good test for the wave functions at the electron-electron coalescence line. The QFM depends on the proper inclusion of correlations of the bound state electrons. It can not be reproduced by uncorrelated bound state functions [7]. The QFM is the only mechanism of ionization which requires going

beyond the dipole approximation since it takes place only if the quadrupole terms in photon-electron interaction are included.

This stimulated us to calculate various characteristics of the double photoionization for the negative ion H^- , He atom and for two-electron ions Li^+ , Be^{++} and B^{+3} with $Z = 3, 4, 5$, respectively in the region of QFM domination at the photon energies $I \ll \omega \ll \mu$. We trace the Z dependence for the double differential distribution. For He we traced the dependence of the photoelectron energy distribution on the photon energy. Since the interest to the QFM renewed recently[9], [14] we hope these data to be useful.

Appendix A

In this Appendix we present the refined formula for calculation of the three-dimensional integral $S_1(q)$ defined by Eq.(26).

Inserting representations (24) into the RHS of Eq.(26), we obtain

$$S_1(q) = N(p_1)N(p_2) \int d^3R e^{i\mathbf{q}\mathbf{R}} {}_1F_1(i\xi_1, 1, ip_1r - i\mathbf{p}_1\mathbf{r}) {}_1F_1(i\xi_2, 1, ip_2r - i\mathbf{p}_2\mathbf{r}) \tilde{\Psi}(R, 0), \quad (\text{A1})$$

where $\tilde{\Psi}(R, 0)$ represents the two-electron wave function (in the ground state) at the electron-electron coalescence line. The integral (A1) can be easily calculated for $\tilde{\Psi}(R, 0)$ presented in the form

$$\tilde{\Psi}(R, 0) = \sum_{j=1}^n C_j \exp(-\lambda_j R). \quad (\text{A2})$$

The Pekeris-like wave functions which we applied [12, 13] do not have the form (A2) at the electron-electron coalescence line. However, fortunately, it is sufficient to include five separate exponential terms ($n = 5$) to obtain extremely accurate wave function $\tilde{\Psi}(R, 0)$ of the form (A2) by fitting the Pekeris-like wave functions with the number of shells $\Omega = 25$ [13].

It follows from Eqs.(A1) and (A2) that calculations of the integral (A1) reduce to computation of the integral

$$I(q, \lambda, s) = \int e^{i\mathbf{q}\mathbf{R} - \lambda R} {}_1F_1(i\xi_1, 1, ip_1r - i\mathbf{p}_1\mathbf{r}) {}_1F_1(i\xi_2, 1, ip_2r - i\mathbf{p}_2\mathbf{r}) R^s d^3R. \quad (\text{A3})$$

It is clear that the analytic form for the latter integral with $s = 0$ can be obtain by differentiation of the integral (A3) with $s = -1$, in respect to parameter λ . The analytic form of the integral $I(q, \lambda, -1)$ was derived in Ref.[15]. Now we employing this result and take into

account that integral (A1) depends, in fact, only on q^2 . The evaluation mentioned above provides the required integral in the form:

$$I(q, \lambda, 0) = -4\pi (\lambda^2 + q^2)^{i(\xi_1 + \xi_2) - 1} (p_2 - p_1 - i\lambda)^{-i\xi_1} (p_1 - p_2 - i\lambda)^{-i\xi_2} (p_1 + p_2 + i\lambda)^{-i(\xi_1 + \xi_2)} \times \left\{ {}_1F_1 [i\xi_1 + 1, i\xi_2 + 1; 2; h(q, \lambda)] \frac{2\lambda\xi_1\xi_2 h(q, \lambda)}{(p_1 - p_2)^2 + \lambda^2} + {}_1F_1 [i\xi_1, i\xi_2; 1; h(q, \lambda)] \times \left(\frac{\xi_1 + \xi_2}{p_1 + p_2 + i\lambda} + \frac{\xi_1}{p_1 - p_2 + i\lambda} + \frac{\xi_2}{p_2 - p_1 + i\lambda} + \frac{2\lambda[i(\xi_1 + \xi_2) - 1]}{\lambda^2 + q^2} \right) \right\},$$

where

$$h(q, \lambda) = 1 - \frac{\lambda^2 + q^2}{(p_1 - p_2)^2 + \lambda^2}. \quad (\text{A4})$$

-
- [1] M. Ya. Amusia, E. G. Drukarev, V. G. Gorshkov, M.P.Kazachkov, J. Phys. B **8**,1248 (1975).
- [2] E. G. Drukarev and F. F. Karpeshin, J. Phys. B. **9**, 399 (1976).
- [3] R. Krivec, M. Ya. Amusia, and V. B. Mandelzweig, Phys. Rev. A **64**, 052708 (2001).
- [4] T. Surić, E. G. Drukarev and R. H. Pratt, Phys. Rev. A**67**, 022709 (2003).
- [5] T. Kato, Commun. Pure Appl. Math **10**, 151 (1957).
- [6] E. Z. Liverts, M. Ya. Amusia, E. G. Drukarev, R. Krivec and V. B. Mandelzweig, Phys. Rev. A **71**, 012715 (2005).
- [7] E. G. Drukarev and A. I. Mikhailov *High Energy Atomic Physics*, Springer International Publishing Switzerland 2016.
- [8] M. S. Schöffler et al. Phys. Rev. Lett. **111**, 0132003 (2013).
- [9] S. Grundmann, V. Serov, F. Trinter, K. Fehre, N. Strenger, A. Pier, M. Kircher, D. Trabert, M. Weller, L. L. Kaiser, A. W. Bray, L. Ph. H. Schmidt, J. B. Williams, T. Jahnke, R. Dorner, M. S. Schoffler, and A. S. Kheifets Physical Review Letters, submitted (2020); arXiv: <https://arxiv.org/abs/2001.07713>
- [10] M. Ya. Amusia, E. G. Drukarev, E. Z. Liverts, and A. I. Mikhailov, Phys. Rev. A **87**, 043423 (2013).
- [11] E. Z. Liverts, M. Ya. Amusia, R. Krivec and V. B. Mandelzweig, Phys. Rev. A **73**, 012514 (2006).
- [12] E. Z. Liverts and N. Barnea, Compt. Phys. Comm. **182**, 1790 (2012).

- [13] E. Z. Liverts and N. Barnea, *Compt. Phys. Comm.* **184**, 2596 (2013).
- [14] S.-G. Chen, W.-C. Jiang, S. Grundmann, F. Trinter, M. S. Schoffler, T. Jahnke, R. Dorner, H. Liang, M.-X. Wang, L.-Y. Peng, and Q. Gong, *Phys. Rev. Lett.* **124**, 043201 (2020).
- [15] A. Nordsieck, *Phys. Rev.* **93**, 785 (1954).

FIG. 1: Distribution $d^2\sigma/d(q^2)d\beta$ in $10^{-10}a_0^4$ is presented as a function of q^2 in a_0^{-2} , where a_0 is the Bohr radius, and $\beta = 0$. The solid lines correspond to the photon energies $\omega = 145, 800, 2000, 3750, 6100$ eV, whereas the dashed lines correspond to the photon energies $\omega = 180, 1000, 2500, 4700, 7600$ eV for H^- , He and helium-like ions with $Z = 3; 4; 5$, respectively.

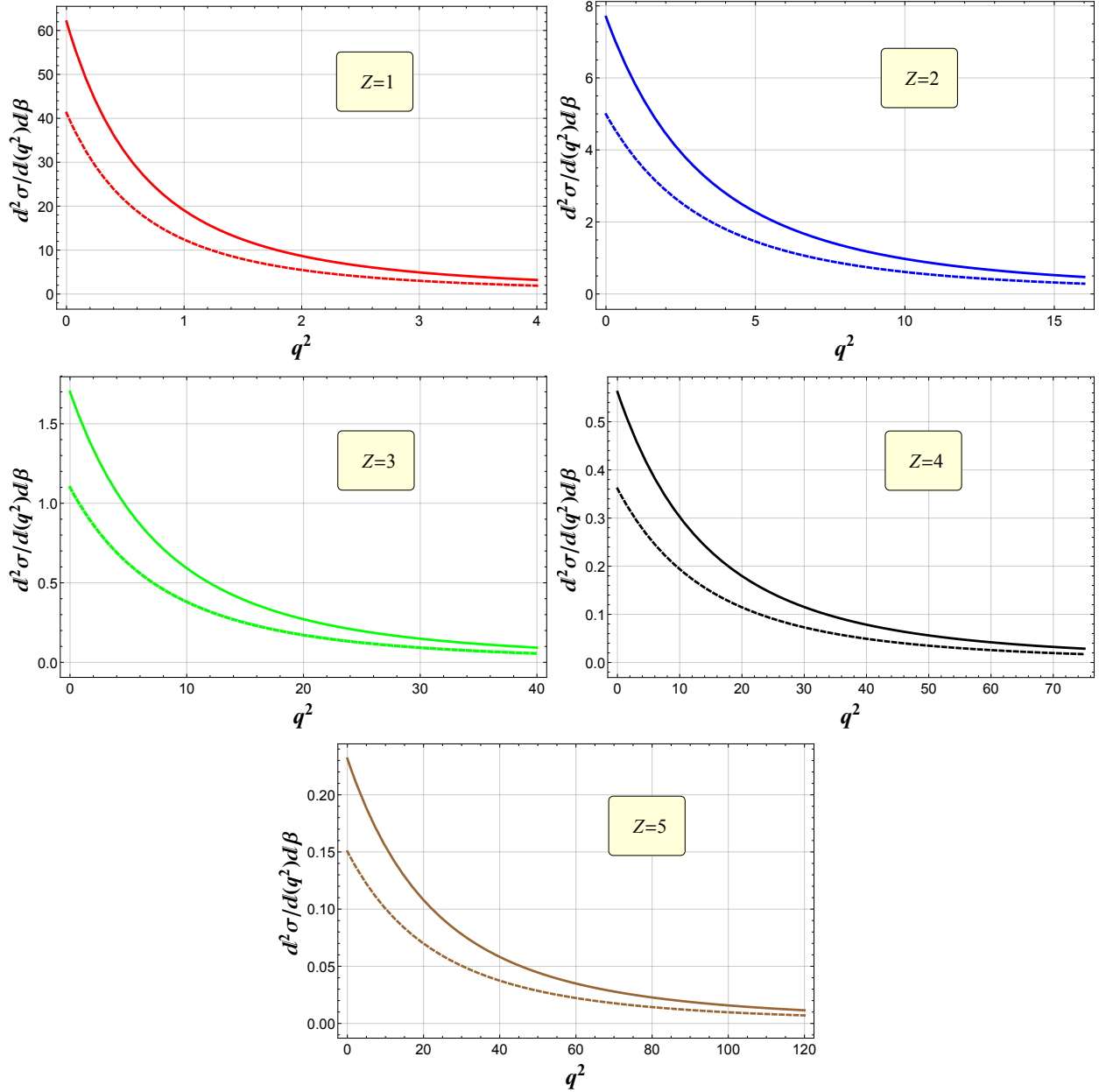


FIG. 2: Distribution $d\sigma/d(q^2)$ in $10^{-10}a_0^4$ is presented as a function of q^2 in a_0^{-2} , where a_0 is the Bohr radius. The solid lines correspond to the photon energies $\omega = 145, 800, 2000, 3750, 6100$ eV, whereas the dashed lines correspond to the photon energies $\omega = 180, 1000, 2500, 4700, 7600$ eV for the helium-like atoms with $Z = 1; 2; 3; 4; 5$, respectively.

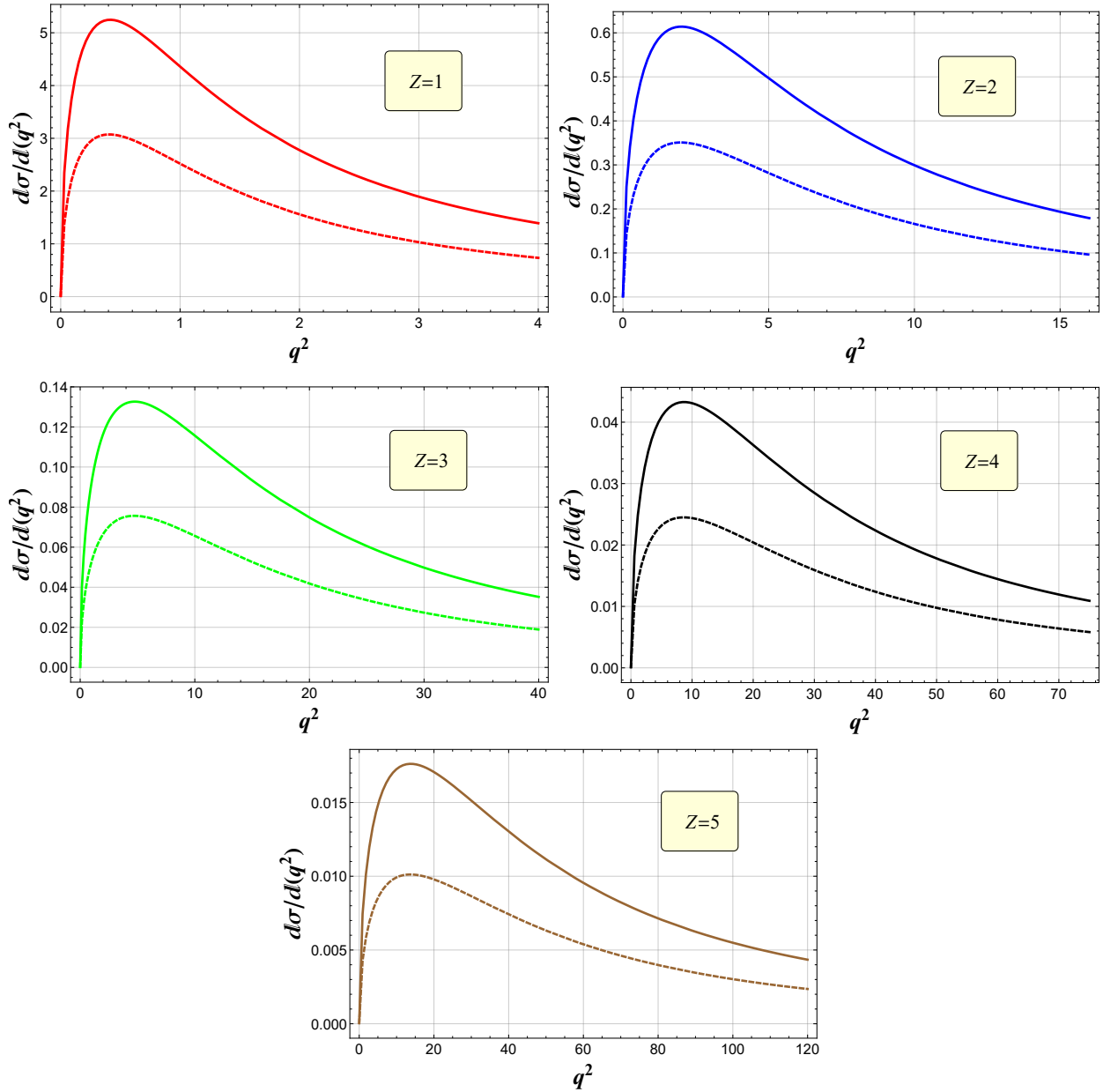


FIG. 3: Distribution $d^2\sigma/d\tau d\beta$ in barns is presented as a function of $\tau = (\mathbf{p}_1 \cdot \mathbf{p}_2)/(p_1 p_2)$ for $\beta = 0$. The curves on the plot (a) correspond to the photon energies $\omega = 145, 800, 2000, 3750, 6100$ eV, whereas the curves on the plot (b) correspond to the photon energies $\omega = 180, 1000, 2500, 4700, 7600$ eV for H^- , He and two-electron ions with $Z = 3; 4; 5$, respectively.

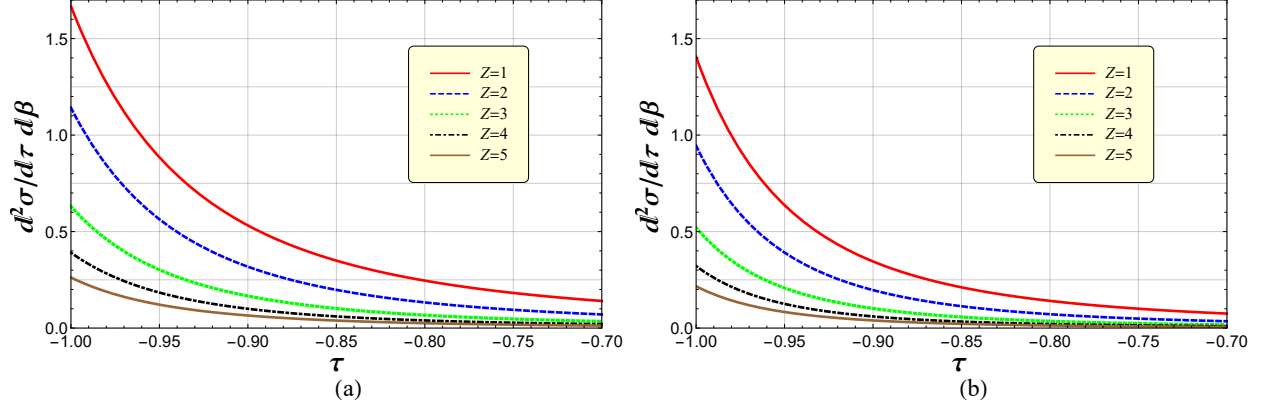


FIG. 4: Distribution $d\sigma/d\tau$ in barns is presented as a function of τ . The curves on the plot (a) correspond to the photon energies $\omega = 145, 800, 2000, 3750, 6100$ eV, whereas the curves on the plot (b) correspond to the photon energies $\omega = 180, 1000, 2500, 4700, 7600$ eV for H^- , He and two-electron ions with $Z = 3; 4; 5$, respectively.

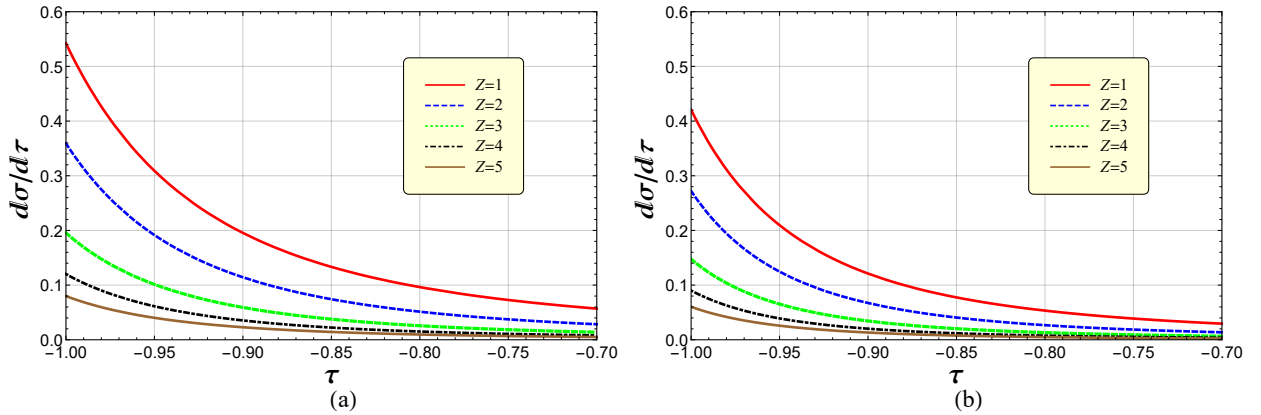


FIG. 5: Distribution $d\sigma/d\beta$ in $10^{-10}a_0^2$ is shown as a function of the photon energy ω (in eV) for the helium-like isoelectronic sequence with $1 \leq Z \leq 5$ (a_0 is the Bohr radius). Only the short ranges of ω containing the photon energies considered in the paper are presented.

